JACC: CARDIOVASCULAR INTERVENTIONS VOL. 18, NO. 21, 2025

PUBLISHED BY ELSEVIER

ORIGINAL RESEARCH

STRUCTURAL

New-Onset Conductance Disturbances After Transcatheter Tricuspid Valve Replacement

A Mechanistic Assessment

Robin Le Ruz, MD,[a,b,c] Tamim Nazif, MD,[c] Isaac George, MD,[c] Elaine Y. Wan, MD,[c] Vratika Agarwal, MD,[c] Mark Lebehn, MD,[d] Carolina Pinheiro Rezende, PA,[c] Joanna Bartkowiak, MD,[c,e] Eun Kyoung Kim, MD, PhD,[c,f] Emily Tat, MD,[c] Vivian Ng, MD,[c] Torsten P. Vahl, MD,[c] Martin B. Leon, MD,[c] Susheel K. Kodali, MD,[c] Rebecca T. Hahn, MD[c]

ABSTRACT

BACKGROUND The anatomical relationship between the tricuspid annulus and the conduction system increases the risk for new-onset conductance disturbance (NOCD) following transcatheter tricuspid valve replacement (TTVR).

OBJECTIVES The aim of this study was to describe the incidence and types of NOCD and potential risk factors.

METHODS This was a single-center, retrospective analysis of TTVR patients. The primary endpoint was 30-day NOCD incidence. Subgroups with (NOCD+) and without (NOCD−) conduction disturbances were compared. Echocardiographic measures of tricuspid valve and right ventricular size, morphology, and function as well as post-TTVR computed tomographic device position within the annulus were assessed.

RESULTS A total of 70 patients were included in this analysis, of whom 31 (44.3%) developed NOCD, which included right bundle branch block, complete atrioventricular block and slow atrial fibrillation. New permanent pacemaker implantation was required in 8 patients (14%) within 30 days. Baseline absolute right ventricle free wall longitudinal strain was significantly higher in NOCD+ patients (29.7% ± 5.4% vs 25.1% ± 6.4%; $P = 0.002$). Type IIIB leaflet morphology was more prevalent in NOCD+ patients (48.4% vs 25.6%; $P = 0.049$). No difference was found regarding membranous septum (MS) dimensions or device oversizing. The postprocedural incidence of white blood cell count peak $>13 \times 10^9$/L was higher in NOCD+ patients (51.6% vs 28.2%; $P = 0.046$). By logistic regression, the primary outcome was associated with baseline absolute right ventricle free wall longitudinal strain ≥29% and contact of subvalvular device component with the MS on follow-up computed tomography.

CONCLUSIONS NOCD incidence was 44.6% after TTVR in a highly selected patient population. Baseline hyperdynamic right ventricular function and contact of the device with the MS were independently associated with NOCD at 30 days. Further studies are warranted. (JACC Cardiovasc Interv. 2025;18:2569-2579) © 2025 by the American College of Cardiology Foundation.

From the [a]Nantes Université, CHU Nantes, Interventional Cardiology Department, l'Institut du Thorax, Nantes, France; [b]Nantes Université, CHU Nantes, CNRS, INSERM, l'Institut du Thorax, Nantes, France; [c]Department of Medicine, Columbia University Irving Medical Center, New York, New York, USA; [d]California Pacific Medical Center, San Francisco, California, USA; [e]Department of Cardiology, University of Bern, Inselspital, Bern, Switzerland; and the [f]Division of Cardiology, Department of Medicine, Cardiovascular Imaging Center, Samsung Medical Center, Sungkyunkwan University School of Medicine, Seoul, Republic of Korea.
The authors attest they are in compliance with human studies committees and animal welfare regulations of the authors' institutions and Food and Drug Administration guidelines, including patient consent where appropriate. For more information, visit the Author Center.

Manuscript received February 19, 2025; revised manuscript received May 26, 2025, accepted July 28, 2025.

ISSN 1936-8798/$36.00 https://doi.org/10.1016/j.jcin.2025.07.039

JACC: CARDIOVASCULAR INTERVENTIONS VOL. 18, NO. 21, 2025
NOVEMBER 10, 2025:2569-2579

ABBREVIATIONS AND ACRONYMS

aRVFWLS = absolute right ventricular free wall longitudinal strain

CT = computed tomography

FAC = fractional area change

HFH = heart failure hospitalization

iRVEDV = indexed right ventricular end-diastolic volume

MS = membranous septum

NOCD = new-onset conductance disturbance

PPI = permanent pacemaker implantation

RV = right ventricle/ventricular

TR = tricuspid regurgitation

TTE = transthoracic echocardiographic

TTVR = transcatheter tricuspid valve replacement

TV = tricuspid valve

WBC = white blood cell

Transcatheter tricuspid valve replacement (TTVR) is a promising device therapy that can address a broad spectrum of tricuspid regurgitation (TR) etiologies and morphologies.[1] Recently, the TRISCEND II trial demonstrated that TTVR with the EVOQUE system (Edwards Lifesciences) resulted in a significant improvement in the composite endpoint of major clinical and quality-of-life outcomes compared with medical therapy.[2] However, it also demonstrated that similar to permanent pacemaker implantation (PPI) rates following surgical tricuspid valve (TV) repair (6%-14%) and replacement (15%-34%),[3-5] the risk for PPI was high after TTVR (17.8% of the whole cohort and 27.8% in pacemaker-naive patients).[2] The anatomical relationship between the tricuspid annulus and the conduction system increases the risk for new-onset conductance disturbances (NOCDs) for both surgical and transcatheter therapies. Recognized risk factors for the need for PPI after TV surgery are female sex, prior sternotomy, and conductance disturbances at baseline.[4] Risk stratification prior to TTVR remains unknown. Given the recent U.S. Food and Drug Administration approval of TTVR in the United States, we sought to study the incidence and spectrum of NOCD and to determine associated risk factors and potential mechanistic causes.

METHODS

This was a single-center, retrospective, observational study of all patients undergoing successful TTVR at Columbia University Medical Center. This research received ethical approval of the local institution (IRB AAAV0931). Procedure indication was defined by the local heart team. Exclusion criteria were pacing dependence at baseline and missing pacer interrogation at follow-up.

PROCEDURE. Patients underwent TTVR following the recommended device instructions-for-use protocols. Device sizing was determined by the device company according to the anatomical features displayed on computed tomography (CT) and transesophageal echocardiography. Postprocedurally, patients were monitored on telemetry during the entire course of their hospitalization (at least 48 hours) and eventually after discharge with mobile outpatient cardiac telemetry.

ENDPOINTS. The primary endpoint of the study was any NOCD noted on telemetry, pacemaker interrogation, or standard 12-lead electrocardiography within 30 days of the procedure. In addition, risk factors independently associated with the occurrence of NOCD were studied, as well as the prognostic impact of NOCD on the composite outcome of all-cause mortality and heart failure hospitalization (HFH).

CLINICAL AND ECHOCARDIOGRAPHIC DATA. All clinical and transthoracic echocardiographic (TTE) data were collected at baseline and first follow-up. TTE assessment of TV anatomy, TR, and right ventricular (RV) function was performed in accordance with Tricuspid Valve Academic Research Consortium.[6] TR etiology was assessed by experienced echocardiographers (R.T.H, M.L, V.A.), according to published consensus requirements. RV free wall longitudinal strain was performed using semi-automated speckle-tracking technology and reported as absolute numbers (absolute RV free wall longitudinal strain [aRVFWLS]). A segmental analysis of RV strain was conducted as previously described by using the left ventricular strain package in TomTec Imaging and applying it to the RV endocardial border to obtain a 6-segment model.[7]

CT. CT was done at baseline and either systematically at the first follow-up visit if renal function allowed (creatinine <2 mg/L) or at other time points if there was a clinical indication. CT was performed using a tricuspid protocol that has been previously described.[8] Membranous septum (MS) length was measured in systole as the distance between the nadir of the noncoronary leaflet and the crest of the interventricular septum. MS width was assessed in end-systole in the "en face" surgical view of the TV, between the superior ridge of the interventricular septum and the anatomical tricuspid annulus. Annular and RV base areas and perimeters were measured in end-systole and end-diastole. RV base was defined as the coaxial plane located 5 mm below the anatomical annulus. Oversizing of the device was calculated according to the formula (Device dimension − Native dimension)/(Native dimension) × 100.

Valve oversizing was assessed in end-systole and end-diastole using multiple measurements: 1) maximal dimensions (septolateral or anteroposterior) of the annulus and RV base; 2) tricuspid annular perimeter; and 3) diameter-derived perimeters of the RV base. The septolateral diameter was defined as the maximal distance of the orthogonal

FIGURE 1 **Computed Tomographic Analysis Methodology**

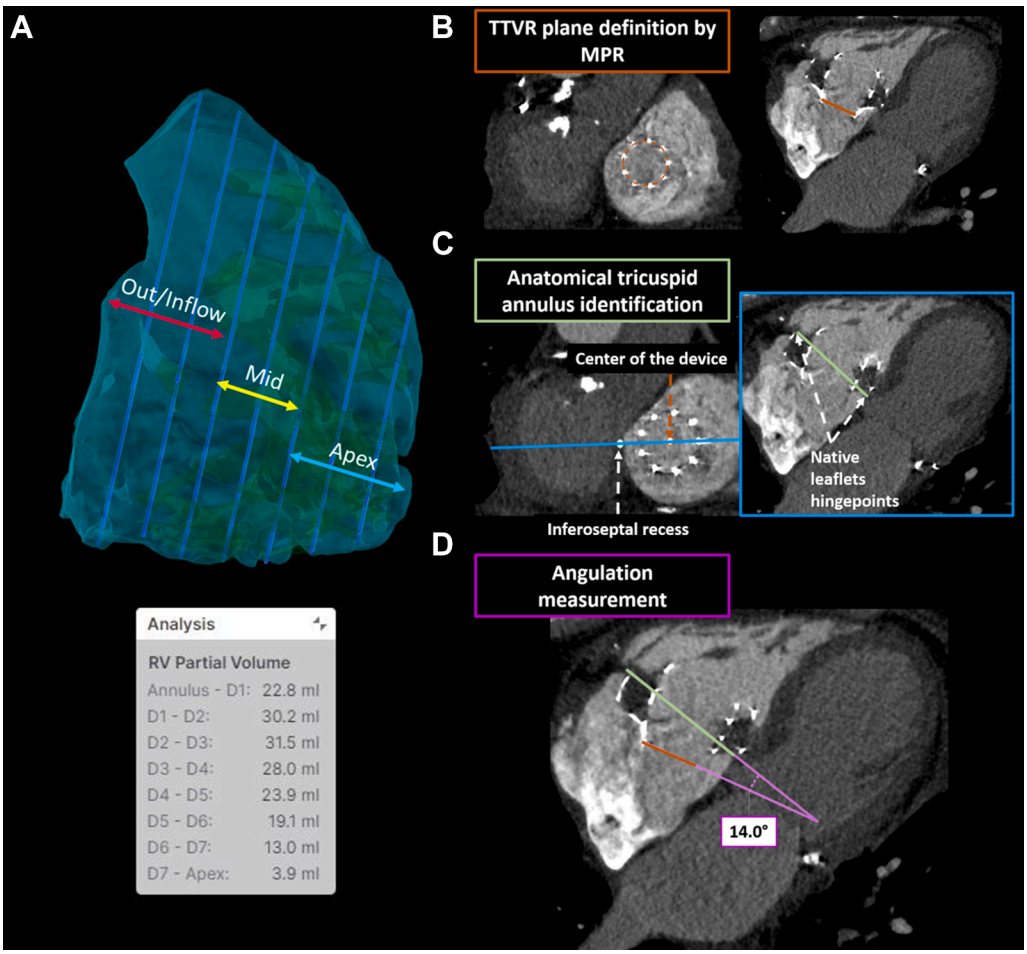

To quantify the relative stroke volume contribution of portions of the right ventricle (RV), the chamber was segmented into 8 partial volumes and analyzed as 3 distinct regions: outflow/inflow, mid, and apex (A). An example of the end-diastolic volumetric quantification of each partial volume is shown. (B) Identification of the device plane (orange line). The axis crossing the center of the device and the inferoseptal recess is used to define the tricuspid annulus (C). From the long-axis view (C, blue box) the tricuspid annular plane is identified as the plane transecting the hinge points of the septal and lateral leaflets (green line). The device orientation angle between these 2 planes, 14.0° in this example, can then be measured. This example shows a septal angulation, given that the device is lower on the septal side (both planes cross on the side of the septum). MPR = multiplanar reconstruction; TTVR = transcatheter tricuspid valve replacement.

axis to the anteroposterior direction. Further analyses were performed using LARALAB software (LARALAB), an artificial intelligence cloud-based platform developed to provide automatic, standardized, and reproducible measurements, including chamber volumetric segmentation and quantification and tricuspid annular and RV dimensions. To better understand the contribution of each region of the RV, the ventricular cavity was divided in 8 equidistant partial volumes, throughout the cardiac cycle (Figure 1A). The 3 more proximal were analyzed as the outflow/inflow region, the 2 in the center represented the midregion, and the 3 distally the apical region. It was then possible to measure the stroke volume of each of them and their relative contribution to the total RV stroke volume.

On post-TTVR CT, the TTVR septolateral plane was first identified (Figure 1B), and the angle of orientation was then defined by identifying the angle between 2 planes: 1) the plane of the device defined by the top of the outer frame (Figure 1B); and 2) the plane transecting the base of the native septal leaflet, located on the inferior margin of the MS at the level of the inferoseptal recess, and opposing lateral leaflet

FIGURE 2 Type and Incidence of NOCD

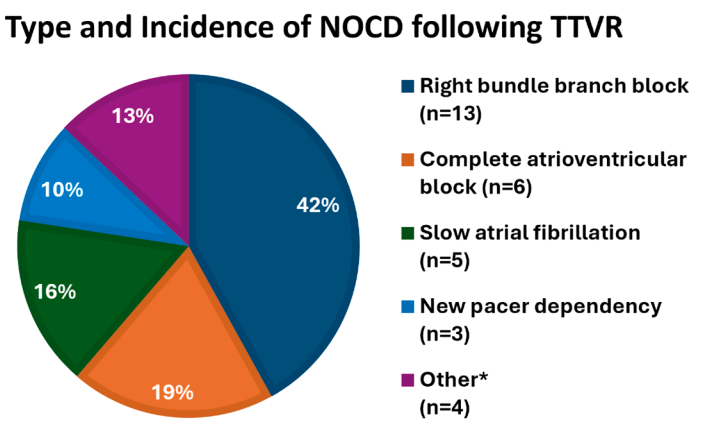

The type and distribution of new-onset conduction disturbances (NOCD) following transcatheter tricuspid valve replacement (TTVR) are shown. The most common NOCD was right bundle branch block in 42% of patients. *Includes atrioventricular block type 1 (n = 1), atrioventricular block type 2 (n = 2), and left posterior fascicular block (n = 1).

hinge point (Figure 1C). The septolateral device angulation was defined as "zero" when both were parallel, "septal" when the subvalvular portion of the device was more ventricular in position along the septum, and "lateral" when the lower part of the device was more ventricular in position along the lateral free wall.

STATISTICAL ANALYSIS. Continuous variables are presented as mean ± SD when the distribution is normal; otherwise presented as median (Q1-Q3). Independent groups are compared using Student's *t*-test or the Wilcoxon-Mann-Whitney rank sum test for normally and non-normally distributed continuous variables, respectively. Categorical data are presented as number (percentage), and comparisons were performed using the chi-square test. Two logistic regression models were built to establish independent correlates of NOCD, one including the whole cohort and the other limited to the patients with available post-TTVR computed tomographic data. A Kaplan-Meier curve was designed for event-free survival assessment, and comparison between groups was made using the log-rank test. All statistical analyses were performed using SPSS software (SPSS).

RESULTS

PATIENT POPULATION. Between 2017 and 2024, 80 patients underwent TTVR. Of those, 10 were excluded, resulting in a total of 70 patients for this analysis (Supplemental Figure 1). Study population had a median age of 81 years (Q1-Q3: 72-84 years), 62.9% were women, 88.6% were in atrial fibrillation or flutter, and 21.4% had prior pacemakers or defibrillators (of those 15 patients, 2 had subcutaneous defibrillators). Patients were highly symptomatic (NYHA functional class III or IV in 53 [75.7%]) and were at high surgical risk, as categorized by the TRI-SCORE (median predicted in-hospital mortality 14%; Q1-Q3: 8%-22%).

At 30-day follow-up, 31 patients (44.3%) met the primary study endpoint. Detailed outcomes are shown in Figure 2. Most frequent events were right bundle branch block, which occurred in 13 patients (41.9%), followed by complete atrioventricular block in 6 individuals (19.4%) and slow atrial fibrillation in 5 subjects (16.1%). The median time between TTVR and NOCD was 1 day (Q1-Q3: 0-3 days), and only 1 patient had a NOCD identified on mobile cardiac outpatient telemetry on day 4. Ultimately, 8 patients underwent PPI, corresponding to an incidence of 11.4% (8 of 70), or 14.0% (8 of 57) when considering PPI-naive patients.

BASELINE CLINICAL CHARACTERISTICS. Baseline characteristics between patients with (NOCD+) and without (NOCD−) are shown in Table 1. NOCD+ and NOCD− patients had similar clinical histories except for less frequent prior sternotomy in the NOCD+ group (32.3% vs 56.4%; $P = 0.044$), in the setting of numerically lower rates of coronary artery revascularization (19.4% vs 33.3%) and left-sided valvulopathy intervention (29.0% vs 48.7%), both statistically nonsignificant. Before the procedure, QRS complexes were narrower in the NOCD+ population (80 ms [Q1-Q3: 80-120 ms] vs 120 ms [Q1-Q3: 80-140 ms]; $P = 0.044$).

ECHOCARDIOGRAPHIC ASSESSMENT. TTE assessment at baseline showed several differences. Although left ventricular and RV global functions (fractional area change [FAC]) did not differ significantly, RV longitudinal function was better in NOCD+ patients: tricuspid annular plane systolic excursion 17 mm (Q1-Q3: 14-19 mm) vs 14 mm (Q1-Q3: 11-17 mm) ($P = 0.051$), S′-wave velocity 10 cm/s (Q1-Q3: 9-11 cm/s) vs 8 cm/s (Q1-Q3: 7-10 cm/s) ($P = 0.002$), and aRVFWLS 29.7% ± 5.4% vs 25.1% ± 6.4% ($P = 0.002$). Regional aRVFWLS analysis (base, mid, and distal) revealed a significantly higher longitudinal strain of the basal segment in the NOCD+ subgroup (37.9% [Q1-Q3: 30.3%-45.2%] vs 30.8% [Q1-Q3: 22.2%-35.4%]; $P = 0.006$), with no differences in mid and distal strain. There were no differences between the NOCD− and NOCD+ subgroups in the incidence of massive or

torrential TR, at 87.2% (n = 34) and 83.9% (n = 26), respectively ($P = 0.694$), or TR etiologies ($P = 0.736$). Nonetheless, valve morphology differed between groups, with type IIIB being more prevalent in the NOCD+ population, at 48.4% (n = 15) vs 25.6% (n = 10) ($P = 0.049$).

COMPUTED TOMOGRAPHIC ASSESSMENT. Preprocedural computed tomographic analysis is reported in Table 2. No specific difference was found in terms of valvular apparatus anatomy, including annular and MS dimensions. No differences were found between the groups for any method of oversizing measurement. However, the volumetric analysis showed that indexed RV end-diastolic volume (iRVEDV) tended to be smaller in the NOCD+ group, and an indexed iRVEDV <120 mL/m^2 was significantly more prevalent in the NOCD+ group (n = 16 [53.3%] vs n = 11 [28.2%]; $P = 0.034$). Consistent with the TTE segmental strain evaluation, the regional volumetric quantification revealed that the outflow/inflow segment had significantly greater contribution to the total RV stroke volume in NOCD+ patients (50.4% [Q1-Q3: 46.5%-52.1%] vs 47.1% [Q1-Q3: 44.6%-50.6%]; $P = 0.041$). A more detailed CT analysis comparing patients with and without type IIIB TV anatomy is provided in Supplemental Table 1. Patients with IIIB morphology had a wider MS (14.2 mm [Q1-Q3: 12.0-16.4 mm] vs 11.2 mm [Q1-Q3: 9.1-13.7 mm]; $P = 0.006$) and greater septolateral angulation of the device on post-TTVR CT (7.1° [Q1-Q3: 4.4°-14.6°] vs 4.4° [Q1-Q3: 1.7°-6.7°]; $P = 0.036$)

PROCEDURAL OUTCOMES. The majority of procedures were performed with the EVOQUE system (n = 54 [77.1%]), the remaining patients from the cohort were treated with 1 of the 3 other TTVR platforms implanted during this period at our institution. Within 48h after the TTVR procedure, a white blood cell (WBC) count peak >13 × 10^9/L was more frequently reported in NOCD+ patients (n = 16 [51.6%] vs n = 11 [28.2%]; $P = 0.046$) (Table 3).

POST-TTVR IMAGING ASSESSMENT. TTE findings after TTVR are shown in Table 4. RV longitudinal function post-TTVR was no longer significantly different between groups, but the reduction in aRVFWLS was significantly greater in NOCD+ patients (−11.9% ± 5.9% vs −5.5% ± 7.5%; $P < 0.001$). FAC similarly showed a greater reduction in NOCD+ patients.

A total of 43 patients of our study population underwent repeat CT, on average 119 ± 255 days post-TTVR; results are shown in Table 5. Following TTVR, RV chambers were markedly smaller in NOCD+ patients; 77.8% (n = 14) of NOCD+ patients had iRVEDV <100 mL/m^2 compared with 41.7% (n = 10) in the NOCD− subgroup ($P = 0.019$). Median septolateral device angulation was similar between

TABLE 1 Baseline Characteristics Comparison Between NOCD− and NOCD+ Groups

	NOCD− (n = 39)	NOCD+ (n = 31)	*P* Value
Demography			
Age, y	81 (70-84)	80 (76-83)	0.822
Female	24 (61.5)	20 (64.5)	0.798
BMI, kg/m^2	24.9 (20.7-27.0)	25.1 (22.2-29.0)	0.527
Clinical history			
Atrial fibrillation	34 (87.2)	28 (90.3)	0.681
Coronary artery revascularization	13 (33.3)	6 (19.4)	0.191
Sternotomy	22 (56.4)	10 (32.3)	0.044
Intervention for left-sided valvulopathy	19 (48.7)	9 (29.0)	0.095
Prior PM or ICD	10 (25.6)	5 (16.1)	0.335
CKD	19 (48.7)	19 (61.3)	0.294
Beta-blockers	30 (76.9)	27 (87.1)	0.277
TRI-SCORE, %	14.0 (7.3-22.0)	14.0 (8.0-22.0)	0.393
Electrocardiographic findings			
PR interval, ms	195 (160-234)	200 (180-260)	0.475
QRS duration, ms	120 (80-140)	80 (80-120)	0.040
Bundle branch block			0.282
Right	14 (35.9)	5 (16.1)	
Left	1 (2.6)	1 (3.2)	
Other intraventricular block			0.804
Nonspecific	7 (17.9)	3 (9.7)	
LPFB	2 (5.1)	2 (6.5)	
LAFB	9 (23.1)	8 (25.8)	
Laboratory results			
WBC count, ×10^9/L	5.82 (4.48-7.68)	6.32 (4.96-8.34)	0.279
Neutrophil/lymphocyte ratio	3.42 (2.32-4.94)	2.73 (1.72-3.93)	0.195
Echocardiography			
LVEF, %	58 (55-62)	59 (55-64)	0.821
Cardiac index, L/min/m^2	2.6 (2.1-3.2)	2.4 (1.8-2.8)	0.187
RV basal diameter, mm	51.0 ± 6.6	50.8 ± 6.3	0.686
RV end-systolic area, cm^2	16.9 ± 4.6	16.4 ± 4.4	0.870
TAPSE, mm	14 (11-17)	17 (14-19)	0.051
S′-wave velocity, cm/s	8 (7-10)	10 (9-11)	0.002
FAC, %	40.6 ± 8.9	39.0 ± 8.8	0.440
aRVFWLS, %	25.1 ± 6.4	29.7 ± 5.4	0.002
Absolute base strain peak, %[a]	30.8 (22.2-35.4)	37.9 (30.3-45.2)	0.006
Absolute mid strain peak, %[a]	26.3 (19.9-32.1)	28.2 (22.1-33.0)	0.429
Absolute apex strain peak, %[a]	23.9 (17.5-32.5)	23.3 (20.2-26.4)	0.809
aRVFWLS >29%	11 (28.2)	18 (58.1)	0.012
RA indexed volume, mL/m^2	74.9 (52.0-97.5)	59.2 (43.8-85.5)	0.048
Massive or torrential TR	34 (87.2)	26 (83.9)	0.694
TV tethering height	9.0 (7.0-10.0)	6.0 (0-11.0)	0.139
TR etiology			0.736
Primary	7 (17.9)	4 (12.9)	
vSTR	9 (23.1)	10 (32.3)	
aSTR	14 (35.9)	12 (38.7)	
CIED	9 (23.1)	5 (16.1)	
TV morphology type IIIB	10 (25.6)	15 (48.4)	0.049

Values are median (Q1-Q3), n (%), or mean ± SD. [a]Left ventricular strain package was used on TomTec to provide segmental analysis of RV strain.

aRVFWLS = absolute right ventricular free wall longitudinal strain; aSTR = atrial secondary tricuspid regurgitation; BMI = body mass index; CKD = chronic kidney disease; CIED = cardiac implantable electronic device; FAC = fractional area change; ICD = implantable cardioverter-defibrillator; LAFB = left anterior fascicular block; LPFB = left posterior fascicular block; LVEF = left ventricular ejection fraction; NOCD = new-onset conduction disturbance; PM = pacemaker; RA = right atrial; RV = right ventricular; S′ = tissue Doppler systolic velocity; TAPSE = tricuspid annular plane systolic excursion; TR = tricuspid regurgitation; TV = tricuspid valve; vSTR = ventricular secondary tricuspid regurgitation; WBC = white blood cell.

TABLE 2 Preprocedural Computed Tomographic Characteristics

	NOCD− (n = 39)	NOCD+ (n = 31)	*P* Value
iRVEDV, mL/m^2	138.9 (109.1-161.4)	115.2 (102.5-141.9)	0.069
iRVEDV <120 mL/m^2	11 (28.2)	16 (53.3)	0.034
iRVESV, mL/m^2	62.0 (46.8-72.0)	55.1 (42.8-61.3)	0.175
iRVSV, mL/m^2	75.0 ± 20.7	65.3 ± 14.9	0.033
RVEF, %	55.7 (50.8-59.7)	56.6 (48.4-59.3)	0.753
% contribution of the outflow/inflow region	47.1 (44.6-50.6)	50.4 (46.5-52.1)	0.041
% contribution of the midregion	29.7 (28.1-31.5)	28.3 (27.3-30.1)	0.030
% contribution of the apical region	22.2 (20.0-24.3)	21.0 (18.4-23.1)	0.245
Indexed end-systolic right atrial volume, mL/m^2	167.2 ± 67.9	145.4 ± 59.0	0.163
End-systolic RA/RV volume ratio	3.0 (2.0-3.8)	2.8 (2.1-3.2)	0.799
Membranous interventricular septum			
Length	6.5 (5.2-8.2)	7.3 (4.8-9.7)	0.804
Width	12.7 (9.2-16.1)	12.3 (9.5-15.4)	0.800
ED annular perimeter	141.6 ± 11.5	144.5 ± 9.9	0.271
ES annular perimeter	133.1 ± 12.4	136.8 ± 11.4	0.205
ED subannular perimeter	195.2 ± 31.0	197.0 ± 21.6	0.750
ES subannular perimeter	150.6 ± 16.9	153.3 ± 18.2	0.527
ED annular oversizing, %: perimeter	8.9 (4.7-11.2)	9.0 (6.1-12.1)	0.696
ES annular oversizing, %: perimeter	14.0 (10.7-18.7)	13.4 (10.3-20.7)	0.965
ED annular septolateral oversizing, %	9.3 (3.6-16.4)	10.0 (5.9-18.3)	0.577
ES annular septolateral oversizing, %	20.9 (14.0-26.3)	19.0 (12.1-30.2)	0.867
ED subannular septolateral oversizing, %	−1.6 (−9.8 to 14.3)	−1.2 (−9.1 to 9.1)	0.887
ES subannular septolateral oversizing, %	24.4 (15.4-34.2)	29.2 (10.7-40.1)	0.972

Values are median (Q1-Q3), n (%), or mean ± SD.

ED = end-diastolic; ES = end-systolic; iRVEDV = indexed right ventricular end-diastolic volume; iRVESV = indexed right ventricular end-systolic volume, iRVSV = indexed right ventricular stroke volume; RVEF = right ventricular ejection fraction; other abbreviations as in Table 1.

both groups, and no specific orientation appeared to be associated with NOCD. The incidence of a contact between the subvalvular part of the device and the MS in end-systole was significantly higher in the NOCD+ group (n = 12 [66.7%] vs n = 6 [24.0%]; $P = 0.005$).

TABLE 3 In-Hospital Clinical Evidence for Inflammation Following Transcatheter Tricuspid Valve Replacement Procedure

	NOCD− (n = 39)	NOCD+ (n = 31)	*P* Value
Fever	10 (25.6)	10 (32.3)	0.543
Peak WBC count within 72 h,×10^9/L	10.6 (9.0-14.2)	13.1 (8.7-15.5)	0.242
WBC count peak >13 × 10^9/L	11 (28.2)	16 (51.6)	0.046
Neutrophil/lymphocyte ratio	11.42 (8.30-19.03)	12.08 (7.31-18.99)	0.962
Variation of WBC compared with baseline, %	79.4 (39.0-125.8)	82.5 (52.3-139.0)	0.504

Values are n (%) or median (Q1-Q3).

Abbreviations as in Table 1.

FACTORS ASSOCIATED WITH NOCD. Logistic regression models were performed to define the independent predictors of the occurrence of NOCD. Model 1 (Table 6A), including the whole study population, showed that aRVFWLS >29% was the only factor presenting a statistically significant association with the primary endpoint (OR: 4.20; 95% CI: 1.30-13.58; $P = 0.017$). Given our population, this analysis was replicated including exclusively EVOQUE valve recipients, and the findings remained unchanged (Supplemental Table 2). Model 2 (Table 6B) is the logistic regression analysis for patients with an available post-TTVR computed tomographic assessment, showing a consistent association with high aRVFWLS and, in addition, suggesting the relevant role of the contact between the subvalvular part of the device and the MS (OR: 7.35; 95% CI: 1.51-35.73; $P = 0.013$) (Central Illustration). In model 3 (Table 6C), excluding patients with prior transvalvular cardiac implantable electronic devices, aRVFWLS remained associated with NOCD, and an additional statistical association with type IIIB TV morphology was also seen.

CLINICAL OUTCOMES. In total, 10 NOCD+ patients required pacing within 30 days, 2 only temporary and 8 permanent. Of the 8 patients who underwent PPI, 6 received coronary sinus leads, 1 with a leadless device and 1 with a conventional RV lead (after leadless implantation failure). At first pacer interrogation (median 21 days), the ventricular pacing rate was 56% (Q1-Q3: 26%-100%), whereas it was only 18% (Q1-Q3: 4.8%-98%) at midterm (median, 275 days).

After a median follow-up period of 619 days (Q1-Q3: 155-963 days), 13 (34.2%) and 11 (35.5%) patients met the composite endpoint of all-cause mortality or HFH in the NOCD− and NOCD+ groups, respectively. Time-to-first event analysis revealed no differences between groups ($P = 0.937$) (Supplemental Figure 2). A Cox proportional hazards analysis resulted in similar findings (HR: 1.37; 95% CI: 0.58-3.25; $P = 0.469$) (Supplemental Figure 3).

DISCUSSION

This mechanistic study aiming to ascertain the incidence and causes of NOCD after TTVR found that: 1) the incidence of NOCD is high, up to 44.3% in our cohort, with a new PPI rate of 14.0%; 2) at baseline, NOCD+ patients displayed hyperdynamic RV longitudinal function but also had fewer prior open heart procedures, with more type IIIB TV morphology;

3) after the procedure, RV remodeling (reduction in size and function) was greater, and WBC count >13 × 10^9/L was more frequent in those presenting with NOCD; 4) on multivariable analysis, baseline TTE aRVFWLS and the presence of device contact with the MS on post-TTVR CT were associated with the primary endpoint of NOCD; and 5) there was no association between NOCD and mortality or HFH at last follow-up.

Although the rate of NOCD was high in this cohort, the new PPI rates are comparable, if not lower, than reported rates in TTVR trials (24.7%),[2] surgical valve replacement (15%-34%),[3-5] or valve repair (6%-14%).[9,10] The surgical literature suggests that patients who needed permanent pacemakers following TV surgery did not have worse long-term survival,[4,10] which is supported by our findings. Of note, surgical patients are by definition at lower risk and, therefore, more frequently younger than TTVR candidates, with less advanced right heart disease and fewer comorbidities.

RV longitudinal function in our cohort was significantly different between NOCD+ and NOCD− subgroups (aRVFWLS 29.7% ± 5.4% vs 25.1% ± 6.4%; $P = 0.002$). This could be related to the statistically higher prevalence of prior sternotomy in the NOCD− population, which is known to be associated with reduced RV longitudinal function, compensated by an improvement in its radial component.[11,12] Whereas global function (both FAC and RV ejection fraction) was preserved and similar between subgroups, our study showed differences in regional contributions to function; NOCD+ patients had significantly higher basal aRVFWLS compared with NOCD− patients (37.9% vs 30.8%; $P = 0.006$). This was consistent with the segmental computed tomographic analysis, which demonstrated a higher contribution to RV stroke volume from the inflow/outflow region in the NOCD+ subgroup (50.4% vs 47.1%; $P = 0.041$), with a smaller contribution from the mid-RV (28.3% vs 29.7%; $P = 0.03$). These findings may help explain the incidence of NOCD, as longitudinal free wall shortening in systole results in longitudinal lateral annular motion with relatively stable septal annular position. In the setting of a semirigid TTVR bioprostheses, the exaggerated "hinge-like" longitudinal motion of the annulus may result in excessive interaction of the subvalvular device structures with the septum and its surrounding structures, including the conduction system. The His bundle travels through the inferior part of the MS before bifurcating into the left and right bundle branches at the muscular interventricular septum crest, the latter emerging and traveling at the septal surface of the RV, downstream the bifurcation. Pathologic studies previously showed that the conduction system pathway travels in those regions that are in close proximity to the implantation site of TTVR devices and, therefore, at risk for injury, particularly in the setting of increased mechanical constraints due to hyperdynamic basal RV shortening.[13]

In addition to RV function implications at the time of implantation, postprocedural RV remodeling may also contribute to NOCD.[14] NOCD+ patients experienced greater reduction in RV function (both aRVFWLS and FAC) and greater RV remodeling with smaller RV end-systolic volume index (51.2 mL/m² vs

TABLE 4 Post-Transcatheter Tricuspid Valve Replacement Echocardiographic Findings

	NOCD− (n = 35)	NOCD+ (n = 28)	*P* Value
RV basal diameter, mm	48.4 ± 6.5	49.7 ± 6.7	0.443
Δ RV basal diameter	−3.1 ± 8.2	−1.1 ± 7.8	0.325
RV end-systolic area, cm²	18.1 (13.9-23.0)	16.1 (14.4-21.4)	0.931
Δ RV end-systolic area	2.1 ± 4.5	2.4 ± 3.6	0.737
TAPSE, mm	12.0 (8.8-15.0)	12.5 (10.9-15.0)	0.561
Δ TAPSE	−1.7 (−7.0 to 1)	−4.0 (−7.0 to 0.2)	0.383
S′-wave velocity, cm/s	7 (6;8)	7 (6;10)	0.350
Δ S′-wave velocity	−1 (−3 to 0)	−2 (−4 to −1)	0.182
aRVFWLS, %	19.9 ± 6.8	18.8 ± 4.3	0.442
Δ aRVFWLS	−5.5 ± 7.5	−11.9 ± 5.9	<0.001
FAC, %	30.7 ± 8.4	24.6 ± 7.4	0.004
Δ FAC	−9.8 ± 9.4	−15.5 ± 10.2	0.024

Values are mean ± SD or median (Q1-Q3).
Abbreviations as in Table 1.

TABLE 5 Post-Transcatheter Tricuspid Valve Replacement Computed Tomographic Analyses

	NOCD− (n = 25)	NOCD+ (n = 18)	*P* Value
iRVEDV, mL/m²	106.2 (84.6-127.9)	92.6 (76.6-99.5)	0.112
iRVEDV <100 mL/m²	11 (44.0)	14 (77.8)	0.027
iRVESV, mL/m²	70.2 (52.5-86.0)	51.2 (43.4-64.0)	0.027
RVEF, %	37.8 (30.8-41.8)	41.1 (35.1-45.7)	0.196
TTVR angulation	6.4 (2.0-10.1)	4.1 (1.9-8.8)	0.506
Angulation orientation			0.945
Zero	1 (4.0)	1 (5.6)	
Septal	9 (36.0)	7 (38.9)	
Lateral	15 (60.0)	10 (55.6)	
Subvalvular anchor in contact with membranous septum in ES	6 (24.0)	12 (66.7)	0.005

Values are mean (Q1-Q3) or n (%).
ES = end-systole; other abbreviations as in Tables 1 and 2.

TABLE 6 Logistic Regression Models

	OR (95% CI)	*P* Value
Model 1		
aRVFWLS >29%	4.20 (1.30-13.58)	0.017
Type IIIB TV anatomy	3.17 (0.98-10.2)	0.054
WBC count peak >13 × 10^9/L	2.92 (0.94-9.09)	0.064
iRVEDV <120 mL/m^2	2.23 (0.73-6.89)	0.161
Model 2		
aRVFWLS >29%	5.96 (1.16-30.65)	0.033
Type IIIB TV anatomy	3.33 (0.62-17.79)	0.159
WBC count peak >13 × 10^9/L	1.89 (0.38-9.38)	0.437
Subvalvular part of the device in contact with the MS in ES	7.35 (1.51-35.73)	0.013
Model 3		
aRVFWLS >29%	5.17 (1.19-22.54)	0.029
Type IIIB TV anatomy	7.15 (1.61-31.74)	0.010
WBC count peak >13 × 10^9/L	3.04 (0.79-11.74)	0.107
iRVEDV <120 mL/m^2	2.48 (0.63-9.67)	0.193

Model 1 includes the entire study population (n = 70). Model 2 includes only patients with available post-transcatheter tricuspid valve replacement computed tomographic studies. Model 3 excludes patients with pre-existing cardiac implantable electronic devices.

ES = end-systole; MS = membranous septum; other abbreviations as in Tables 1 and 2.

70.2 mL/m^2; $P = 0.027$), contributing to an increased device-annulus interaction and pressure on the conduction system. Finally, along with these spatial constraints, our findings of greater subannular device contact with the MS support a direct interaction of components of the device structures and the conduction system. Considering this finding, we expected to observe a greater angulation of the device, particularly lateral, resulting in a higher position on the septal side, toward the inferior margin of the MS where the branching component of the conduction axis is. The lack of significant difference between groups in our study may be due to the small population or other anatomical determinants such as conduction system location or valvular morphology.

A number of other possible predictors were not significantly related to NOCD in our study. Device oversizing was not a risk factor in our study. This is likely related to the highly compliant and nonfibrous tricuspid annulus.[15] We had postulated that atrial secondary TR patients could have a higher risk for NOCD given the lack of leaflet tethering. Although we did not find any difference in etiologic classification of TR between NOCD groups, this may be related to the difficulty in distinguishing between etiologies with the current proposed criteria.[6,16] In patients without prior cardiac implantable electronic devices, type IIIB morphology was a significant predictor of NOCD+ along with aRVFWLS. Although we did not find greater subvalvular device interaction with the MS in this morphology, compared with non-IIIB morphologies, patients with IIIB morphology had a wider MS and a more septolateral angulation of the device, both of which may predispose greater interaction of the device along the length of the conduction system. One could postulate this finding to be part of a congenital disease spectrum involving both MS embryogenesis and leaflet formation.[17] Finally, patients after TTVR presented with a significant increase in WBC count within 72 hours. By choosing arbitrarily a cutoff of 13 × 10^9/L, we found that an elevation beyond that threshold was more frequent in the NOCD+ group than among control subjects (51.6% vs 28.2%; $P = 0.049$). Acute inflammation and NOCD have been extensively studied, and mechanistic pathways have been described to possibly explain the link between those 2 entities.[18,19] Either as a local phenomenon caused by the implantation-induced myocardial injury or as a consequence of the systemic release of biomarkers, inflammation could play a role in the occurrence of NOCD in our population. This was also suggested by the change in pacing seen during follow-up with rates decreasing to <20% ventricular pacing at mid-term, perhaps as inflammation resolves. TTVR devices are much larger than any of the other valvular bioprosthesis currently available in clinical practice. In the postprocedural period, exposure to this foreign body may trigger an activation of the immune system, as possibly reflected by the elevated WBC count in our study.[20] Prior reports in the field of transcatheter aortic valve replacement have reported significant, albeit lesser than in our population, WBC elevation post-procedurally.[21] It was even established that this acute inflammatory response differed between the 2 devices most frequently used in clinical practice.[22] This latter finding is consistent with the foreign body-host theory, suggesting that the larger the device surface that is in contact with blood, the greater the activation of the innate immune system. Indeed, WBC elevation was more pronounced in self-expanding platforms, whose design includes more biological tissue given their supra-annular position. The role of inflammation in conduction abnormalities following transcatheter device therapy is supported by a recent study of patients undergoing transcatheter aortic valve replacement, where the use of colchicine resulted in a significant reduction in NOCD.[23]

STUDY LIMITATIONS. This was a single-center analysis including a relatively small population and, therefore, is hypothesis generating. Follow-up CT was not performed in all patients, thus introducing a possible selection bias. By design, patients in the NOCD+ group had fewer conduction disturbances at

CENTRAL ILLUSTRATION New Onset Conduction Disturbance After TTVR

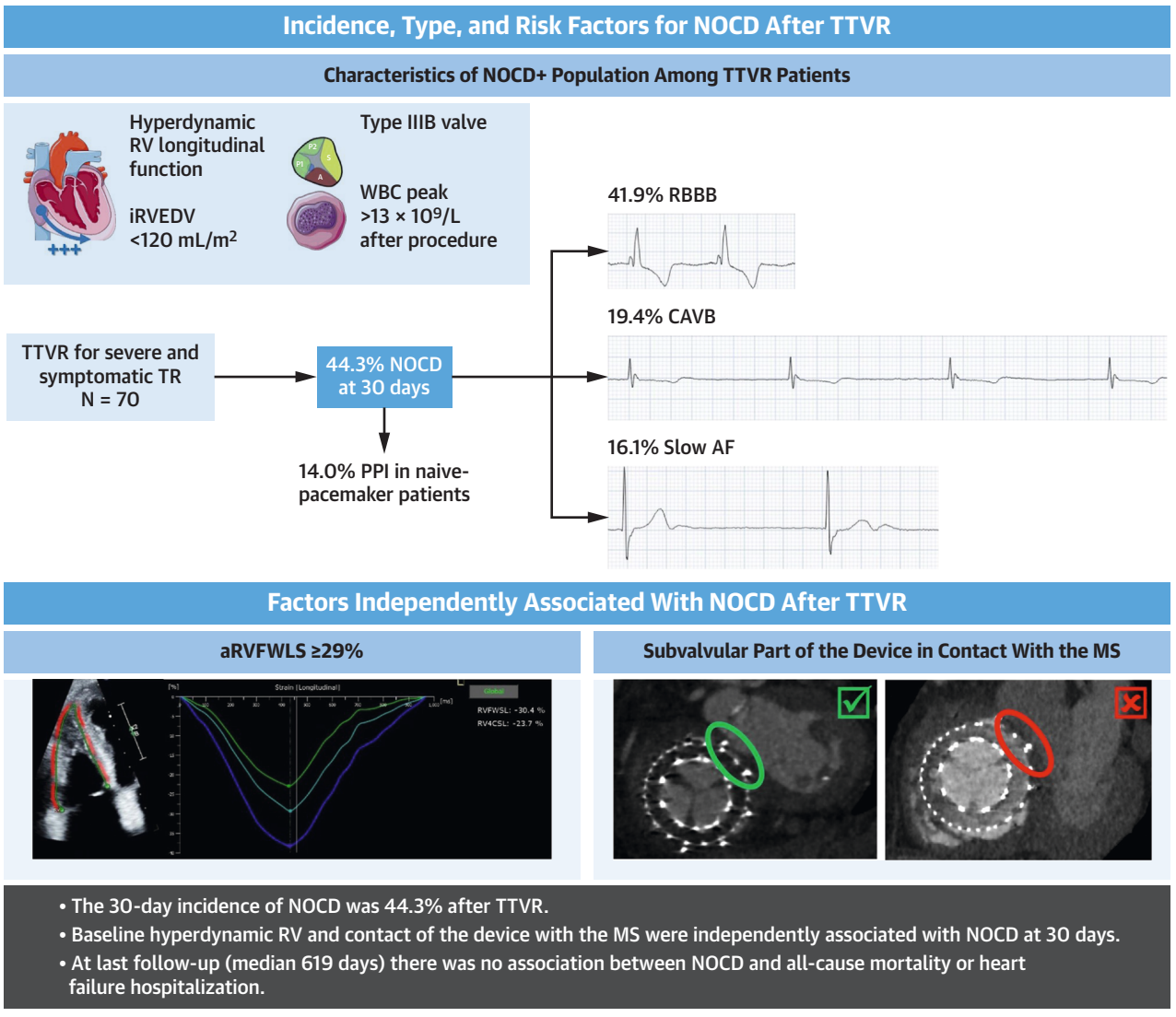

Le Ruz R, et al. JACC Cardiovasc Interv. 2025;18(21):2569-2579.

On the basis of 2 different logistic regression models, main risk factors for new-onset conduction disturbance (NOCD) after transcatheter tricuspid valve replacement (TTVR) were absolute right ventricular free wall longitudinal strain (aRVFWLS) ≥29% at baseline and the contact between the subvalvular part of the device and the membranous septum (MS) on post-TTVR computed tomography. AF = atrial fibrillation; CAVB = Complete atrioventricular block; iRVEDV = indexed right ventricular end-diastolic volume; PPI = permanent pacemaker implantation; RBBB = right bundle branch block; RV = right ventricular; TR = tricuspid regurgitation; TV = tricuspid valve; WBC = white blood cell.

baseline, making them more prone to develop new abnormalities in comparison with those with conduction defects before the procedure. The majority of NOCDs were new right bundle branch block, so patients with pre-existing right bundle branch block (who were not excluded from this analysis) were less likely to meet the primary endpoint of the study. We limited the detection of NOCD to within 30 days of the procedure and there may be late NOCD that was therefore not captured. The majority of patients received 1 device platform, which may significantly affect the analysis of anatomical risk predictors as well as the incidence of NOCD, which may be applicable only to this platform. Our angulation

assessment was restricted to the septolateral direction and may vary depending on the 3-dimensional shape of the tricuspid annulus. Despite these limitations, this report provides a unique multimodality imaging assessment of TTVR recipients, evaluating possible predictors of NOCD.

CONCLUSIONS

NOCD incidence 30 days after TTVR is high, up to 44.3%, mostly due to right bundle branch block and complete atrioventricular block. NOCD+ patients had hyperdynamic RV longitudinal function at baseline and tended to also present with smaller RV cavities and greater postprocedural inflammatory response. On post-TTVR CT, the contact between the subvalvular part of the device and the MS was independently associated with the primary endpoint. Those findings are hypothesis generating and warrant further study.

ACKNOWLEDGMENTS The authors thank Russell Brandwein, Maureen Gaine, Antoine Addoumieh, Jason Bloom, Kevin Gu, Lauren Ranard, and Abdulrahman Museedi for their valuable contributions. The authors are grateful to LARALAB for their support.

FUNDING SUPPORT AND AUTHOR DISCLOSURES

Dr Le Ruz's research fellowship was funded by Fédération Française de Cardiologie, Groupement Interrégional de la Recherche Clinique et de l'Innovation Grand Ouest, the Franco-American Fulbright Program, the Monahan Foundation, Centre Hospitalo-Universitaire de Nantes, and the Columbia University Irving Medical Center Interventional Cardiology Department. Dr Nazif has received institutional funding to Columbia University Irving Medical Center from Medtronic, Boston Scientific, and Edwards Lifesciences; and has received consulting fees from Medtronic, Boston Scientific, and Edwards Lifesciences. Dr George has received consulting fees from Cardiomech, Mitre Medical, AtriCure, VDyne, Valcare Medical, DurVena, MITRx, and Johnson & Johnson. Dr Wan is funded by National Institutes of Health grant R01HL152236 and has been a consultant for Boston Scientific, Medtronic, Cardiologs, and Sanofi. Dr Vahl has received institutional funding to Columbia University Irving Medical Center from Boston Scientific, Edwards Lifesciences, JenaValve, and Medtronic; and has received consulting fees from Abbott Vascular, 4C Medical, InnovHeart, and Philips. Dr Leon has received institutional clinical research grants from Abbott, Boston Scientific, Edwards Lifesciences, Medtronic, and JenaValve. Dr Kodali has received grant support, paid to his institution, from Medtronic, Boston Scientific, and Abbott Vascular; has received consulting fees from Abbott Vascular, Claret Medical, Admedus, and Meril Life Sciences; and holds equity options in BioTrace Medical, Dura Biotech, and Thubrikar Aortic Valve. Dr Hahn has received speaker fees from Abbott Structural, Baylis Medical, Edwards Lifesciences, Medtronic, Philips Healthcare, and Siemens Healthineers; has held institutional consulting contracts for which she receives no direct compensation from Abbott Structural, Edwards Lifesciences, Medtronic, and Novartis; and is chief scientific officer for the Echocardiography Core Laboratory at the Cardiovascular Research Foundation for multiple industry-sponsored TV trials, for which she receives no direct industry compensation. All other authors have reported that they have no relationships relevant to the contents of this paper to disclose.

ADDRESS FOR CORRESPONDENCE: Dr Rebecca T. Hahn, Columbia University Medical Center, NewYork-Presbyterian Hospital, 177 Fort Washington Avenue, New York, New York 10032, USA. E-mail: rth2@columbia.edu. X handle: @hahn_rt.

PERSPECTIVES

WHAT IS KNOWN? NOCDs after TTVR are not infrequent, with prior studies showing a high incidence of new pacemaker requirements.

WHAT IS NEW? In the present study, NOCD following TTVR was associated with baseline hyperdynamic RV longitudinal function and the contact between the subvalvular component of the device and the MS.

WHAT IS NEXT? Understanding predictors of NOCD following TTVR may inform risk prediction algorithms or risk mitigation strategies but requires further study in larger population samples.

REFERENCES

1. Hausleiter J, Stolz L, Lurz P, et al. Transcatheter tricuspid valve replacement. *J Am Coll Cardiol*. 2025;85:265-291.

2. Hahn RT, Makkar R, Thourani VH, et al. Transcatheter valve replacement in severe tricuspid regurgitation. *N Engl J Med*. 2025;392:115-126.

3. Chen Q, Bowdish ME, Malas J, et al. Isolated tricuspid operations: the Society of Thoracic Surgeons Adult Cardiac Surgery Database analysis. *Ann Thorac Surg*. 2023;115:1162-1170.

4. Kassab J, Harb SC, Desai MY, et al. Incidence, risk factors, and outcomes associated with permanent pacemaker implantation following tricuspid valve surgery. *J Am Heart Assoc*. 2024;13:e032760.

5. Alqahtani F, Berzingi CO, Aljohani S, Hijazi M, Al-Hallak A, Alkhouli M. Contemporary trends in the use and outcomes of surgical treatment of tricuspid regurgitation. *J Am Heart Assoc*. 2017;6:e007597.

6. Hahn RT, Lawlor MK, Davidson CJ, et al. Tricuspid Valve Academic Research Consortium definitions for tricuspid regurgitation and trial endpoints. *J Am Coll Cardiol*. 2023;82:1711-1735.

7. Badagliacca R, Reali M, Poscia R, et al. Right intraventricular dyssynchrony in idiopathic, heritable, and anorexigen-induced pulmonary arterial hypertension: clinical impact and reversibility. *JACC Cardiovasc Imaging*. 2015;8:642-652.

8. Pulerwitz TC, Khalique OK, Leb J, et al. Optimizing cardiac CT protocols for comprehensive acquisition prior to percutaneous MV and TV repair/replacement. *JACC Cardiovasc Imaging*. 2020;13:836-850.

9. Gammie JS, Chu MWA, Falk V, et al. Concomitant tricuspid repair in patients with degenerative

mitral regurgitation. *N Engl J Med*. 2022;386:327–339.

10. Ragnarsson S, Taha A, Nielsen SJ, et al. Pacemaker implantation following tricuspid valve annuloplasty. *JTCVS Open*. 2023;16:276–289.

11. Tamborini G, Muratori M, Brusoni D, et al. Is right ventricular systolic function reduced after cardiac surgery? A two- and three-dimensional echocardiographic study. *Eur J Echocardiogr*. 2009;10:630–634.

12. Tokodi M, Nemeth E, Lakatos BK, et al. Right ventricular mechanical pattern in patients undergoing mitral valve surgery: a predictor of postoperative dysfunction? *ESC Heart Fail*. 2020;7:1246–1256.

13. Sanchez-Quintana D, Anderson RH, Tretter JT, Cabrera JA, Sternick EB, Farre J. Anatomy of the conduction tissues 100 years on: what have we learned? *Heart*. 2022;108:1430–1437.

14. Weckbach LT, Stolz L, Chatfield AG, et al. Right ventricular reverse remodeling after transcatheter tricuspid valve replacement in patients with heart failure. *J Am Coll Cardiol*. 2023;81:708–710.

15. Yamane K, Takahashi Y, Fujii H, et al. Histology of the tricuspid valve annulus and right atrioventricular muscle distance. *Interact Cardiovasc Thorac Surg*. 2022;35:ivac175.

16. Muraru D, Badano LP, Hahn RT, et al. Atrial secondary tricuspid regurgitation: pathophysiology, definition, diagnosis, and treatment. *Eur Heart J*. 2024;45:895–911.

17. Allwork SP, Anderson RH. Developmental anatomy of the membranous part of the ventricular septum in the human heart. *Br Heart J*. 1979;41:275–280.

18. Lazzerini PE, Abbate A, Boutjdir M, Capecchi PL. Fir(e)ing the rhythm: inflammatory cytokines and cardiac arrhythmias. *JACC Basic Transl Sci*. 2023;8:728–750.

19. Lazzerini PE, Acampa M, Cupelli M, et al. Unravelling atrioventricular block risk in inflammatory diseases: systemic inflammation acutely delays atrioventricular conduction via a cytokine-mediated inhibition of connexin43 expression. *J Am Heart Assoc*. 2021;10:e022095.

20. Morris AH, Stamer DK, Kyriakides TR. The host response to naturally-derived extracellular matrix biomaterials. *Semin Immunol*. 2017;29:72–91.

21. Condado JF, Junpaparp P, Binongo JN, et al. Neutrophil-lymphocyte ratio (NLR) and platelet-lymphocyte ratio (PLR) can risk stratify patients in transcatheter aortic-valve replacement (TAVR). *Int J Cardiol*. 2016;223:444–449.

22. Abu Khadija H, Gandelman G, Ayyad O, et al. Differential systemic inflammatory responses after TAVI: The role of self versus balloon expandable devices. *PLoS One*. 2021;16:e0258963.

23. Ryffel C, Lanz J, Guntli N, et al. Colchicine in patients with aortic stenosis undergoing transcatheter aortic valve replacement: a double-blind randomized trial. *Nat Commun*. 2025;16(1):6501.

KEY WORDS computed tomography, conduction disturbance, echocardiography, transcatheter tricuspid valve replacement

APPENDIX For supplemental tables and figures and a video of the interactive Central illustration, please see the online version of this paper.